3D Stellar Evolution
ASP Conference Series, Vol. 293, 2003
S. Turcotte, S. C. Keller, & R. M. Cavallo, eds.

arXiv:astro-ph/0306151v1 6 Jun 2003

Djehuty, a Code for Modeling Stars in Three Dimensions

G. Bazán, D. S. P. Dearborn, D. D. Dossa, P. P. Eggleton, A. Taylor, J. I. Castor, S. Murray, K. H. Cook, P. G. Eltgroth, R. M. Cavallo, S. Turcotte, S. C. Keller, and B. S. Pudliner

Lawrence Livermore National Laboratory, Livermore CA, 94550

Abstract. Current practice in stellar evolution is to employ one-dimensional calculations that quantitatively apply only to a minority of the observed stars (single non-rotating stars, or well detached binaries). Even in these systems, astrophysicists are dependent on approximations to handle complex three-dimensional processes like convection. Understanding the structure of binary stars, like those that lead to the Type Ia supernovae used to measure the expansion of the universe, are grossly non-spherical and await a 3D treatment.

To approach very large problems like multi-dimensional modeling of stars, the Lawrence Livermore National Laboratory has invested in massively parallel computers and invested even more in developing the algorithms to utilize them on complex physics problems. We have leveraged skills from across the lab to develop a 3D stellar evolution code, Djehuty (after the Egyptian god for writing and calculation) that operates efficiently on platforms with thousands of nodes, with the best available physical data (opacities, EOS, etc.). Djehuty has incorporated all basic physics for modeling stars including an accurate equation of state, radiation transport by diffusion, thermonuclear reaction rates, and hydrodynamics, and we have begun testing it in a number of applications.

1. Why do stellar modeling in three dimensions?

The best determinations of the size, age and composition of the universe are founded on measurements of stars, combined with a physical understanding based on one-dimensional (1D) computations. 1D calculations quantitatively apply only to a minority of the observed stars (single non-rotating stars, or well detached binaries). Even in these systems, astrophysicists are dependent on 1D approximations to complex three-dimensional (3D) processes like convection.

Observations assure us that our best 1D approximation of steady state convection is flawed, requiring ad hoc 'overshoot' corrections. Even worse, there is no real ability to model the time-dependent convection that may be critical in modeling helium flashes, Cepheid and Mira pulsations, or the nucleosynthesis in deep mixing events that follow thermal pulses. In addition, nearly half of the visible mass of the universe is incorporated into intrinsically 3D binary stars, many of which interact significantly at some stage of evolution. Understanding integral properties such as the chemical evolution, or the detailed pre-explosion

structure, of metric phenomena like type Ia supernovae awaits development of a true 3D stellar evolution code.

Developing a 3D code capable of modeling stars is exceedingly challenging. In spite of the inherent difficulty, the importance of obtaining a better understanding of stars has led a small number of groups to begin such work. Most current calculations are practically limited to of order 1 million zones, and cannot realistically handle whole stars (in 3D). Envelope convection has been simulated by modeling modest segments of a star (Clement 1993; Ludwig, Jordan, & Steffen 1994; Freytag, Ludwig, & Steffen 1996; Brummell, Hurlburt & Toomre 1996, 1998; Stein & Nordlund 1998; Skartlien, Stein, & Nordlund 2000; Nordlund & Stein 2001; Porter & Woodward 2000). Quite reasonably, these simulations often lack physical processes pertinent to the core (nuclear energy production), or radiation transport, and the gravitational potential is an imposed condition. While these are important starts toward understanding convection in stars, it is clear that some problems (e.g. solar rotation) yield results that are dependent on the size of the segment that can be simulated (Robinson & Chan 2001), necessitating whole star modeling.

With the advent of massively parallel computers and the development of algorithms able to operate in such a partitioned environment, it became possible to consider developing a code, Djehuty, capable of following meshes with sizes of order 10^8 cells and with a more complete suite of physics. Djehuty is capable of modeling complete stars in three dimensions. It is based on the ALE (Arbitrary Lagrange-Eulerian) hydrodynamic method with a predictor-corrector Lagrange-Remap formalism, that is second-order accurate in both time and space. It supports energy transport, via a pair of diffusion equations, one for matter conduction, and another for radiation. The mesh, constructed of multi-block logically rectangular hexahedrons, is allowed to be non-orthogonal and can conform to the developing instabilities, providing a more accurate tracking. Djehuty permits domain decomposition for parallel operation, using MPI message passing.

The physical data in Djehuty is identical to that used in the 1D evolution code that provides initial structure models. It has an equation of state based on the work of Eggleton, Faulkner & Flannery (1973), as updated by Pols et al. (1995; hereinafter PTEH), that is very accurate for stellar compositions over a large range of masses ($> 0.5\,M_\odot$). Both Planck and Rosseland mean opacities for radiation diffusion come from OPAL (Rogers & Iglesias 1992) and are augmented by Alexander opacities (Alexander & Ferguson 1994) for the lower temperatures where molecules are significant. The nuclear reaction network includes reactions for hydrogen, helium, and carbon burning, and the nuclear reaction rates come from Caughlan & Fowler (1988). Nuclear energy production can also be computed by a tabular set of reactions. Neutrino losses are in tabular form from the work of Itoh et al. (1989, 1992, with errata).

The gravity implementation is currently complete only for spherical stars, but is adequate to begin scientific investigation of a host of issues related to convection. In the coming year, we will implement a generalized gravity solver to study rapidly rotating or binary stars. We are still learning how to improve operational efficiency, but have begun a set of large scale, full physics, parallel runs aimed at our first science objective, the structure of convective cores in high mass main sequence stars.

2. The Physics in Djehuty

2.1. An Astrophysical Equation of State

As an analytic approximation, the PTEH equation of state (EOS) provides continuous thermodynamic derivatives for hydrodynamic consistency. This EOS has been modified to reproduce tabulated OPAL values to an accuracy of better than 1% for the entire range of conditions expected in stars from 0.7 to 50 $M_\odot$ (over their whole evolution). Stellar models as low as 0.5 $M_\odot$ can be computed, with differences of only about 2% in their envelopes.

A comparison of the difference between the OPAL tables and the PTEH EOS is shown in Figure 1. Over most of the temperature-density plane, the difference is under a percent. The upper left corner of the diagram is the region of complete degeneracy (relativistic and non-relativistic), important for white dwarfs, and the cores of red giants. While OPAL tables were not calculated there, the thermodynamics of this region is well represented by the Fermi relations with which the PTEH EOS is in excellent agreement. The upper right hand corner is included in the OPAL tables but without the inclusion of relativistic effects. Here the PTEH code is presumably more accurate, and the difference shown as green and red contours arise from a limitation in OPAL calculations.

Between the degenerate and non-degenerate regions there is a difficult region where Coulomb corrections to the pressure are very significant. This shows as a diagonal band of blue contours where the OPAL and PTEH EOS's differ by more than 1%. It is a region occupied by brown dwarfs, and very low mass stars ($\lesssim 0.5\,M_\odot$), and we will improve agreement there if we decide to investigate such objects in the future.

Successfully transferring a hydrostatic model to Djehuty (with minimal transients) requires that both codes utilize the same EOS. The PTEH EOS has been inserted into Djehuty and tested on a set of two and three dimensional problems as well as our 3D stellar model. In a simple hydrodynamics problem, the accurate EOS call can be a substantial component of the time. The time cost of using this accurate equation of state was minimized by implementing a sub-cycling procedure as well as a method improving the convergence rate of the algorithm. We have been able to optimize the run time of the EOS without sacrificing the accuracy of the results. From the first crude implementation of the accurate EOS, a five-fold speed up has been achieved.

This EOS includes the formation of molecular hydrogen and ionization states of low-Z elements. While the EOS is able to operate on elements up to iron, it is implemented to consider only ^{1}H, ^{3}He, ^{4}He, ^{12}C, ^{14}N, ^{16}O, ^{24}Mg.

2.2. Radiative Diffusion

Energy transport via diffusion is an excellent approximation when the cells of the mesh are optically thick ($\tau \gg 1$ in a zone), a condition that is very well met throughout a star's interior. Djehuty uses a pair flux-limited diffusion equations to approximate energy transport. Included in the diffusion equation are sources and sinks that link the radiation equation to the hydrodynamic energy and momentum equations, as well as nuclear energy production, or neutrino losses. Djehuty operates in a two-temperature (2T) mode, in which the temperatures of the matter and of the radiation field are integrated separately, and the radiation

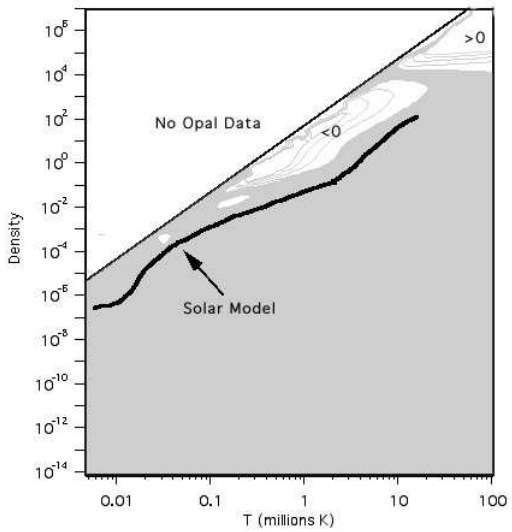

Figure 1. The thick contours mark regions of no difference between the analytic PTEH equation of state, and LLNL tabular values. The grey region marks regions where they differ by $< 1\%$. The diagonal line tracks the temperature density profile of a solar model.

is approximated as Planckian. Again, this is an excellent approximation within stellar interiors, and will enable us to transition to stellar atmospheres. These equations are:

$$\text{radiation}: \quad \frac{\partial \phi}{\partial t} = \nabla.\,(\frac{c}{3\kappa_r \rho}\,\nabla\phi) + \kappa_p \rho c(aT^4 - \phi) + E_\phi \tag{1}$$

$$\text{matter}: \quad \rho C_v \frac{\partial T}{\partial t} = \nabla.\,(D\,\nabla T) + \kappa_p \rho c(\phi - aT^4) + E_m \quad . \tag{2}$$

Here a is the usual radiation constant, ϕ is the radiation energy density per unit volume (which would be aT^4 in complete equilibrium), and E_ϕ, E_m are contributions to the radiation and matter energies from compression, nuclear reactions etc. D is the heat transport coefficient by conduction alone.

Within a star, the matter and radiation are so strongly coupled that the matter and radiation temperatures are essentially identical. This strong coupling is achieved because of the large value for the Planck opacity, κ_p. A table of Planck opacities has been constructed from data from the Opacity Project (Seaton et al. 1994) at high temperatures and of Alexander & Ferguson (1994) at low temperatures. Accurate Planck opacities will be important near the surface where the diffusion approximation becomes poor.

The transfer of radiation is governed by the Rosseland mean opacity, κ_r. Currently Djehuty reads κ_r from a set of astrophysical opacity tables that were formed using OPAL (Livermore) opacities at high temperatures ($> 10,000$ K) and Alexander opacities at lower temperatures where molecules are important

(Alexander & Ferguson 1994; Rogers & Iglesias 1992). This is the same opacity set used by the 1D evolution code. These astrophysical opacities will be the only option actually used in the stellar calculations done by Djehuty, but an analytic Kramer's form for the Rosseland mean opacity is available to facilitate comparisons with other codes.

The radiation package of Djehuty has been given some simple tests to ensure accuracy. The first was a simple Marshak wave problem. A temperature source was applied to one end of a tube. With hydrodynamic motions turned off, and a constant opacity applied, the results can be compared directly with theory. Excellent agreement was found, providing direct evidence that the radiation diffusion package in Djehuty functions well.

2.3. Thermonuclear Rates and Neutrino Losses

Elements normally carried directly by the 1D evolution code were selected to allow accurate tracking of principal energy generation reactions for hydrogen, helium and carbon burning over the whole range of stellar masses. This list of elements includes ^{1}H, ^{3}He, ^{4}He, ^{12}C, ^{14}N, ^{16}O, ^{24}Mg. These elements are passed to Djehuty as part of the mapping process, and form a standard 7-element set.

The 7-element set is an excellent approximation for circumstances of stable hydrogen burning in most stars. It includes the slower hydrogen burning reactions of the PP1 and PP2 chains as well as the CNO cycles. Over evolutionary time-scales, many reactions in the PP chain and CNO Cycles come to equilibrium, and do not need to be specifically included.

The rate equations for the 7-element set are identical to those used in the 1D code and Djehuty integrates those rates with the abundances to determine local energy production and transmutation rates. In this mode, energy production computed by Djehuty and the 1D code are well matched. The rate equations used by Djehuty and the 1D code include not just hydrogen burning, but the most important energy production rates from helium burning and carbon burning stages. We have also included strong and weak Coulomb screening.

Both Djehuty and the 1D code have been written to permit easy expansion of the element set. Djehuty can also operate with an 18-element set suitable for situations where the hot CNO cycle operates. The program is now structured such that it is trivial to add new rates connecting existing elements. It is also relatively easy to increase the element sets when circumstances require.

Operation of the new version is independent of the order in which the elements are specified in the input deck, and the solution of all rate equations is implicit. In tests, the hydrogen mass fraction can be changed by orders of magnitude in a single step. As part of these changes the EOS was modified to handle an arbitrary element set.

In both element sets, the proton-proton chain is handled as follows: the proton capture on deuterium, $\mathrm{p(p,}\beta\,\nu\mathrm{)D(p,}\gamma\mathrm{)}^{3}\mathrm{He}$, is assumed to be followed instantly by $^{3}\mathrm{He}(^{3}\mathrm{He,2p})^{4}\mathrm{He}$ and $^{3}\mathrm{He}(^{4}\mathrm{He},\gamma)^{7}\mathrm{Be(p,}^{4}\mathrm{He)}^{4}\mathrm{He}$.

In the 7-element set, only the slower rates are included in the CNO cycle. The beta decay and proton capture on ^{13}C, $^{12}\mathrm{C(p,}\gamma)^{13}\mathrm{N}(\beta,\nu)^{13}\mathrm{C(p,}\gamma)^{13}\mathrm{N}$, are assumed to be instantaneous. The beta decay and proton capture on ^{15}N, $^{14}\mathrm{N(p,}\gamma)^{15}\mathrm{O}(\beta,\nu)^{15}\mathrm{N(p,}\alpha)^{12}\mathrm{C}$, are also assumed to be instantaneous, as are the beta decay and proton capture on ^{17}O, $^{16}\mathrm{O(p,}\gamma)^{17}\mathrm{F}(\beta,\nu)^{17}\mathrm{O(p,}\alpha)^{14}\mathrm{N}$.

All CNO rates are included in the 17-element suite making it suitable for the hot CNO cycle, including leakage into ^{19}F. They are:

$$^{12}\mathrm{C}(\mathrm{p},\gamma)^{13}\mathrm{N},\ ^{13}\mathrm{N}(\beta,\nu)^{13}\mathrm{C},\ ^{13}\mathrm{C}(\mathrm{p},\gamma)^{14}\mathrm{N},\ ^{14}\mathrm{N}(\mathrm{p},\gamma)^{15}\mathrm{O},\ ^{15}\mathrm{O}(\beta,\nu)^{15}\mathrm{N},$$
$$^{15}\mathrm{N}(\mathrm{p},\alpha)^{12}\mathrm{C},\ ^{15}\mathrm{N}(\mathrm{p},\gamma)^{16}\mathrm{O},\ ^{16}\mathrm{O}(\mathrm{p},\gamma)^{17}\mathrm{F},\ ^{17}\mathrm{F}(\beta,\nu)^{17}\mathrm{O},\ ^{17}\mathrm{O}(\mathrm{p},\alpha)^{14}\mathrm{N},$$
$$^{17}\mathrm{O}(\mathrm{p},\gamma)^{18}\mathrm{F},\ ^{18}\mathrm{F}(\beta,\nu)^{18}\mathrm{O},\ ^{18}\mathrm{O}(\mathrm{p},\alpha)^{15}\mathrm{N},\ \text{and}\ ^{18}\mathrm{O}(\mathrm{p},\gamma)^{19}\mathrm{F}.$$

The following helium burning reactions are also included: ^{4}He(2α,γ)^{12}C, ^{12}C(α,γ)^{16}O, ^{14}N(α,γ)^{18}O, and ^{18}O(α,γ)^{22}Ne. In the 7-element set, the last reaction is assumed to happen instantaneously, and the mass fraction change is placed with all other heavy elements in ^{24}Mg.

Finally, the following reactions are included for beginning advanced stages of massive star evolution: ^{12}C(^{12}C,γ)^{24}Mg and ^{16}O(^{16}O,γ)^{32}S.

As a result, the 7-element set uses 12 reaction rates and the 18-element set evaluates 23 rates. These rates are all evaluated from equations following the form of Harris et al. (1983) and returned as reactions per mole per second. How the reactions are used is defined by three numbers returned for each rate that specify the number of input particles, of output particles, and the number of particles in reaction. This permits the code to include appropriate factors for true multi-body rates like the triple-alpha rate. It also allows two-body rates, like ^{12}C(p,γ)^{13}N, to be correctly evaluated while reducing the number of protons by 2 in the approximation where the reactions ^{13}N(β,ν)^{13}C(p,γ)^{14}N are assumed instantaneous.

Each rate also includes the net energy produced from the rate (less any neutrino energy). This information is used along with the rates to derive the energy production rate in ergs per gram per second. A table for neutrino losses (Itoh et al. 1989, 1992) from Compton, bremsstrahlung, and pair production processes has been included, and is initialized along with the basic data for the EOS routine. The temperature and density are then used to interpolate in this table to provide a neutrino loss rate.

Finally, Djehuty can be quickly transformed by providing the rates in tabular form. We have generated a table using rates associated with the 7-element set and shown good correspondence in energy production and transmutation rates. The tabular method can be implemented without recompiling Djehuty, and lends itself to quick tests. In the future we anticipate using it to simulate chemical rates for modeling giant planet atmospheres.

2.4. Gravity

At present we have implemented a simple algorithm to compute the gravity of a spherical object. Between hydrodynamic cycles, Djehuty integrates over all cells of the mesh to determine a mass-radius relation. In parallel operation, this requires sharing a relatively small amount of information among the processors to construct the relation for the entire star.

Once the spherical mass distribution has been found, the gravitational acceleration can be simply calculated at each node. This method is limited to spherical objects, but its implementation identified much of the process that must occur for a more general treatment to be implemented.

As an extension of this self-consistent spherical gravity, it is possible to add a point mass outside of the problem, and study tidal modification of the model.

This approximation is appropriate only when the star is sufficiently centrally condensed that the portions of the star that are distorted are of modest mass.

2.5. Hydrodynamics

Djehuty uses an ALE (Arbitrary Lagrange-Eulerian) hydrodynamic method, in which an explicit hydrodynamic step is followed by an advection step. In stable regions, or regions of large-scale coherent motion where the Lagrangian mesh is modestly deformed, no advection is necessary, and the code is essentially Lagrangian. In regions where shear develops, it is necessary relax the mesh, and permit material to move between cells.

To promote hydrodynamic accuracy, and time centering for other physical processes, the hydrodynamic step is split in half. The first sub-step is a simple explicit step. This is followed by a second sub-step in which information from both the original position, and information from the half (sub) step position, are used in a predictor-corrector formalism. This allows a time-centered inclusion of radiation transport and energy production with a hydrodynamics step that is second-order accurate in both time and space. In Djehuty, vector quantities like position and velocity are zone-centered, while scalar quantities (density, temperature ...) are cell-centered. By splitting the hydrodynamic step, the node and cell quantities have the same time.

3. Model Generation

3.1. The Initial Models

We developed a 1D stellar evolution code for use as a platform to test physics, and to provide structure information to Djehuty for constructing 3D models. Djehuty reads the 1D stellar evolution models directly, and converts the model into its own variable set. The evolution code follows the work of Eggleton (1972) and has a fully implicit algorithm that includes mesh motion during a time step. This speeds the calculation and improves its accuracy, but results in an unusual centering of the thermodynamic variables. To minimize any transients, software was also written to adjust (and relax) the variables to values appropriate for cell-centered equations used by Djehuty.

As an example the 1D code is capable of following a $4\,M_{\odot}$ model from a pre-main-sequence configuration through main sequence, giant, and thermally pulsing stages to becoming a white dwarf (Figure 2). At any stage of evolution, a restart file can be written that is usable by either Djehuty or the 1D code itself.

As a first test of Djehuty, a pre-main-sequence model of a star approaching the main sequence was tested. At this point, nuclear reactions are negligible ($E_{nuc}/E_{grav} < 0.005$), the composition homogeneous, and the star is almost entirely stable. This model was selected so as to test the accuracy of our scaling and mapping algorithms as well as to test various 3D mesh structures.

A second model that was selected for an initial test case was of a star that has just reached the main sequence. It has a convective core of about $0.4\,R_{\odot}$ (2.8×10^{10}cm), driven by the strong temperature sensitivity of CNO nuclear burning. In this model (Figure 3), carbon has been converted into nitrogen,

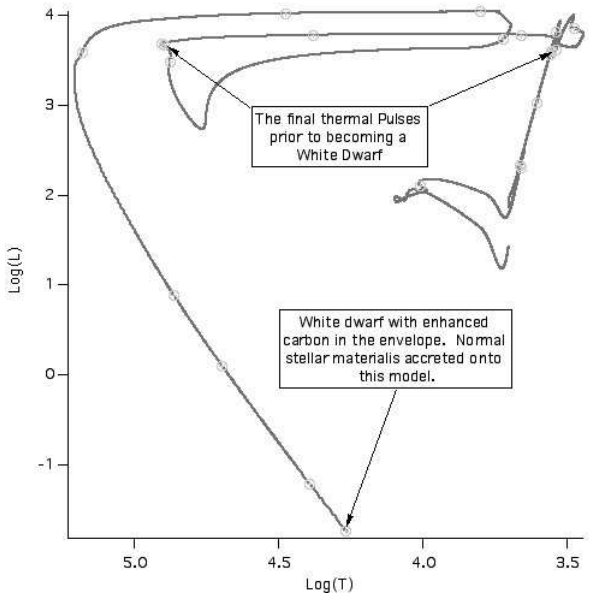

Figure 2. An HR diagram shows the temperature luminosity evolution of a $4\,M_{\odot}$ star from the pre-main-sequence to a point where its remnant core has become a white dwarf. The model positions are shown by open circles.

the core ^{3}He has been destroyed, and the central hydrogen mass fraction has fallen from 0.7 to 0.676. This model has been used to test the nuclear energy generation rates as implemented in Djehuty.

3.2. Mesh Structure

In order to reduce the problem of tiny zones (and time steps), inherent in a mesh using spherical coordinates, we are utilizing a technique in which the sphere is constructed from 7 logical blocks. There is a central block, and 6 adjacent blocks, one attached to each face of the central block. The mesh in each of the outer blocks is morphed to form a spherical tile. The central block can remain as a cube or be morphologically distorted from near rectangular cells at the center to a sphere at its surface. Preliminary numerical experiments suggest that allowing the central block to retain most of its cubic shape results in a better-behaved structure, and smaller deviations from hydrostatic equilibrium (particularly at the corner nodes of the central cube).

As an example (Figure 4), we show a sample logical structure in which the central block (0) is constructed from a mesh with 50x50x50 cells (51x51x51 nodes). There are then 6 additional blocks (1-6), having 50x50x100 cells. In each case, the axis oriented in the radial direction has 100 zones (101 nodes). Blocks 1, 2, and 3, attach to the faces on which the logical variables i, j, and k are 1, while blocks 4, 5, and 6 attach to the faces where i, j, and k have their maximum values.

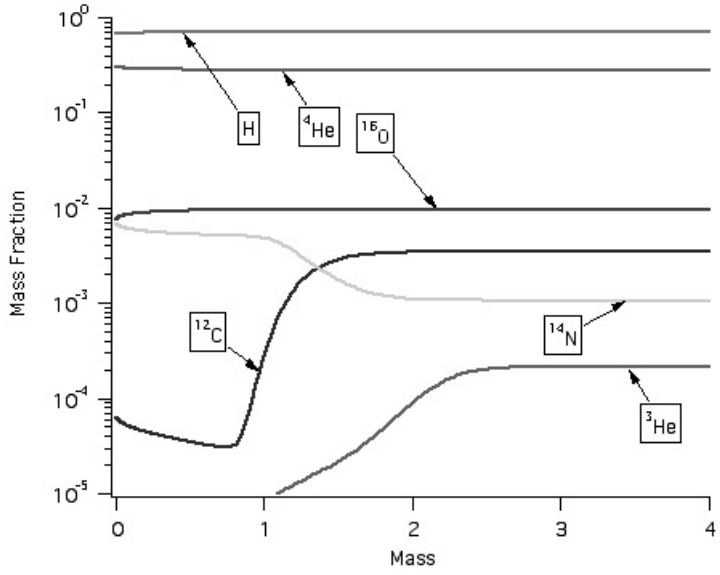

Figure 3. The composition structure of an early main sequence star of $4\,M_{\odot}$.

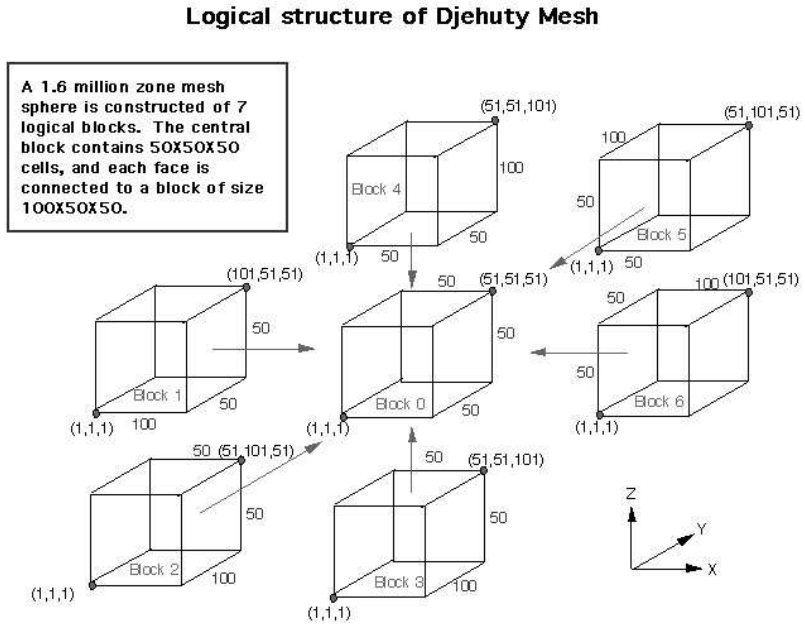

Figure 4. Logical structure of Djehuty mesh.

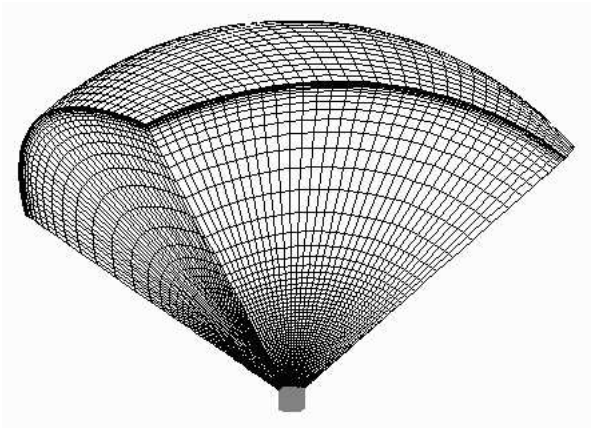

Figure 5. The structure of a representative mesh with 590K zones

The logical (surface) blocks that attach to the central cube must (at present) have the same mesh size as the face to which they adjoin, but the radial component may have any length. These surface blocks are transitioned from a cubic shape to spherical segments (Figure 5). An initial mesh is generated with a standard size. It can then be tailored to a particular stellar model (radius and radial zoning structure). The scaling must not just match the radius of the star, but have a radial spacing to resolve important gradients. The radial structure of the 1D mesh is used as an initial guide for scaling the 3D mesh, but the user has an ability to bias the mesh through a parameter.

This additional flexibility is provided by producing a scale factor that is parameterized as 'grid_scale_alpha'. The scale factor, S_r, was just defined as

$$S_r = r^{\alpha} \tag{3}$$

where r is the fractional radius of a node in the mesh. Setting grid_scale_alpha to a value of 1 results in a direct mapping of the radial structure from the 1D model to the 3D mesh. A value of grid_scale_alpha greater than 1 concentrates the mesh in the core, and makes the envelope sparser. Alternatively a value less than 1 enlarges the core and refines the envelope (Figure 6).

Once the mesh has been scaled, the 1D model is mapped into it. The cells of the small meshes that we have used for our initial testing are of such a size that 3 or 4 of the 1D radial zones contribute to the properties of the cells. Furthermore, the cells near the core will not (in general) have a radial orientation. A simple mapping of zone-centered values led to a cumulative error in total stellar mass that was unacceptably large. This mapping problem was solved by subdividing our 3D cells and integrating the 1D model across the smaller volume elements (Figure 7). The segment masses and volumes were then summed to determine the average cell density. Other properties were then mass-averaged among the segments.

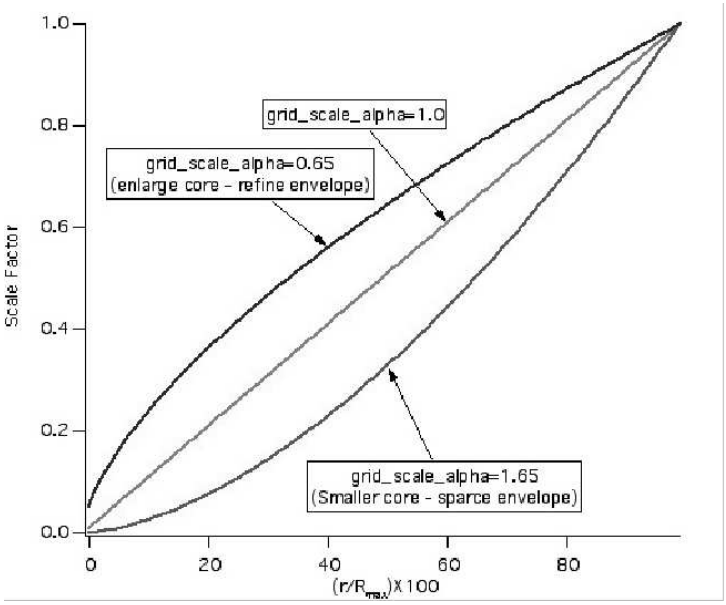

Figure 6. In a coarse 3D mesh, 3 to 4 radial zones from the 1D model may contribute to the properties of a cell.

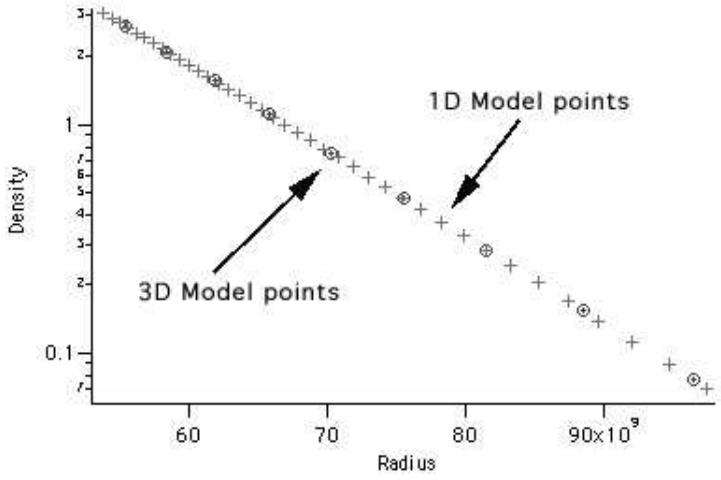

Figure 7. Comparison of 1D model to Djehuty mesh.

4. Model Settling

Figure 8 gives an example of the initial velocity perturbations that result from the mapping of a $4\,M_{\odot}$ model to a 3D mesh. The model is generated with a fixed boundary condition, and run for 5 cycles to an elapsed time of 0.074416 seconds. The grey scale ranges from 0 to 500 cm/s.

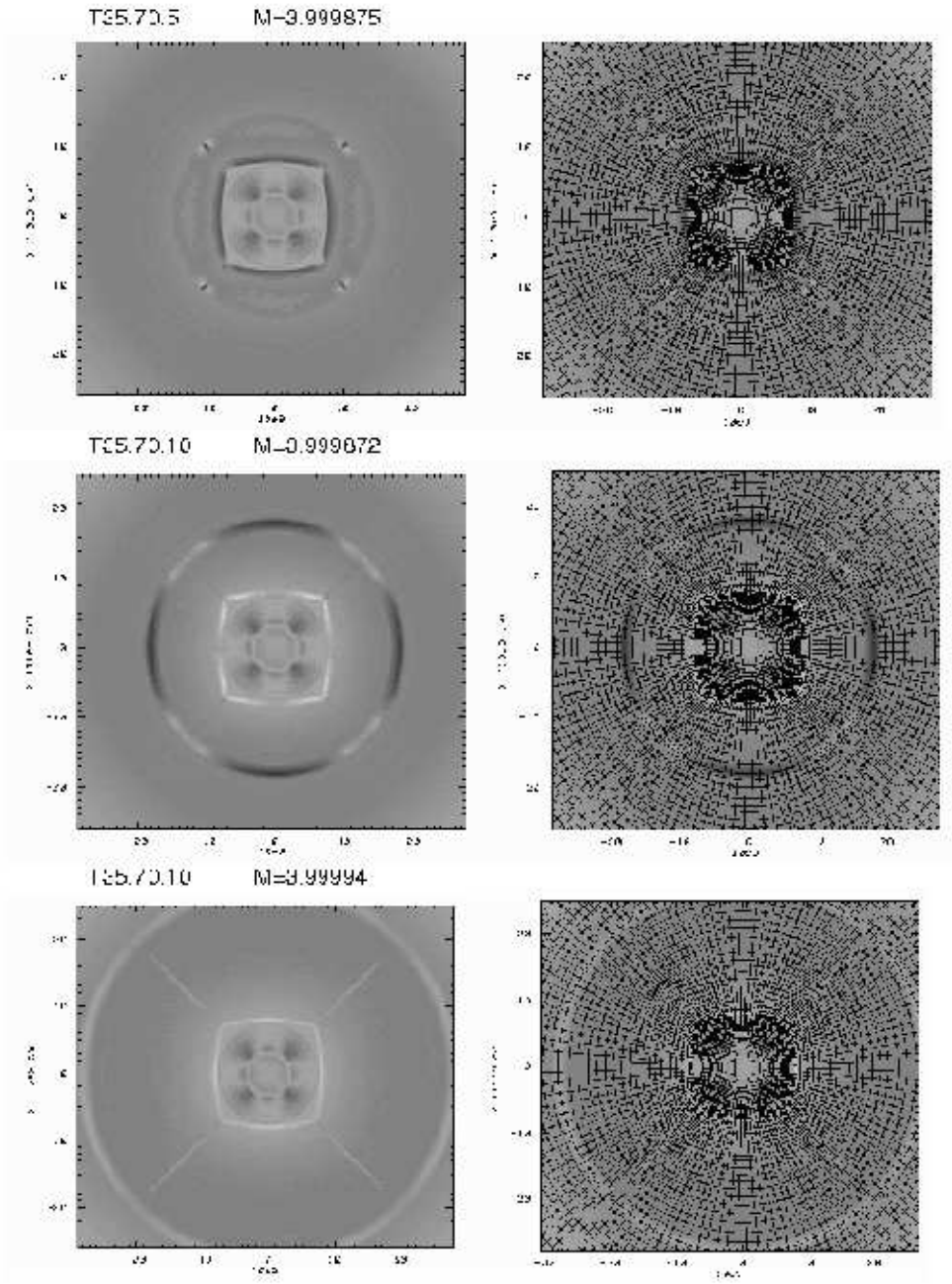

Figure 8. Mesh structures. The initial velocity transients are minimized when the transition region is smoother.

5. Conclusion

Djehuty is now an operational code, and papers are in preparation on stellar simulations that have been made with it (see Figure 3 of Eggleton et al. in these proceedings). Highlights of these calculations include the first 3D simulation of a type II supernova. The nickel produced in the silicon-burning region of these stars is an important energy source in the observed light curves. In SN1987a, it appeared much sooner that expected from a 1D model. Our 3D calculation shows the development of an instability causing tendrils of nickel to extrude into surrounding material, where it appears early, as seen by observers. We have also done a first simulation of a nova. Novae are explosive events that occur in binary-star systems where hydrogen is being torn from a normal star and deposited on to a white dwarf companion. In our first 3D calculation, the hydrogen ignition propagated from a number of ignition points, and created a shock that accelerated the surface to near 3000 km/s. When the shock emerges at the surface, it is heated to temperatures in excess of 1 Kev, creating an X-ray pulse. In this first calculation, the white dwarf mass is a bit smaller that those thought appropriate for most novae, and the hydrogen accretion was symmetric over the surface of the star. A more realistic hydrogen distribution in which the material is settled on to the star as a high velocity stream will be a future calculation. Simulating stable stars, like our $4\,M_\odot$ main sequence model, has been remarkably challenging, but with new boundary conditions the numerical stability problems that precludes long runs seem to have been resolved.

Acknowledgments. This work was performed under the auspices of the U.S. Department of Energy, National Nuclear Security Administration by the University of California, Lawrence Livermore National Laboratory under contract No. W-7405-Eng-48.

References

Alexander, D. R., & Ferguson, J. W. 1994, ApJ, 437, 879

Brummell, N. H., Hurlburt, N. E., & Toomre, J. 1996, ApJ, 473, 494

Brummell, N. H., Hurlburt, N. E., & Toomre, J. 1998, ApJ, 493, 955

Caughlan, G. R., & Fowler, W. A. 1988, in Atomic Data and Nuclear Data Tables, Vol. 40, 283

Clement, M. J. 1993, ApJ, 406, 651

Eggleton, P. P. 1972, MNRAS, 156, 361

Eggleton, P. P., Faulkner, J., & Flannery, B. P. 1973, A&A, 23, 325

Freytag, B., Ludwig, H.-G., & Steffen, M. 1996, A&A, 313, 497

Harris, M. J., Fowler, W. A., Caughlan, G. R., & Zimmerman, B. A. 1983, ARA&A, 21, 65

Itoh, N., Adachi, T., Nakagawa, M., Kohyama, Y., & Munakata, H. 1989, ApJ, 339, 354

Itoh, N., Mutoh, H., Hikita, A., & Kohyama, Y. 1992, ApJ, 395, 622

Ludwig, H.-G., Jordan, S., & Steffen, M. 1994, A&A, 284, 105

Nordlund, Å, & Stein, R. F. 2001, ApJ, 546, 576

Pols, O., Tout, C. A., Eggleton, P. P., & Han, Zh. 1995, MNRAS, 274, 964
Porter, D. H., & Woodward, P. R. 2000, ApJS, 127, 159
Robinson, F. J., & Chan, K. L. 2001, MNRAS, 321, 723
Rogers, F. J., & Iglesias, C. A. 1992, ApJ, 401, 361
Seaton, M. J., Yan, Y., Mihalas, D., & Pradhan, A. K. 1994, MNRAS, 266, 805
Skartlien, R., Stein, R. F., & Nordlund, Å 2000, ApJ, 541, 468
Stein, R. F., & Nordlund, Å 1998, ApJ, 499, 914